Elastoplastic Solution to Spherical Cavity Expansion and Calculation of Penetration Resistance for the Miniature Penetrometer Test

Wei Bai[1,2,3(✉)], Ling-wei Kong[1], Chen Chen[1], and Cheng-sheng Li[1]

[1] State Key Laboratory of Geomechanics and Geotechnical Engineering, Institute of Rock and Soil Mechanics, Chinese Academy of Sciences, Wuhan, China
William_bai@yeah.net
[2] GuangXi Key Laboratory of Geomechanics and Geotechnical Engineering, Guilin University of Technology, Guilin 541004, China
[3] Key Laboratory of Soft Soil Engineering Characteristics and Engineering Environment of Tianjin, Tianjin 300381, China

Abstract. The miniature penetrometer tests are often used to investigate the distribution and strength of aggregates in soils. In this work, the elastoplastic solution to spherical cavity expansion for stress distribution in saturated clay is studied using the cavity expansion theory in combination with the modified Cambridge clay (MCC) model. From the case study, it can be found that the radial stress, circumferential stress and tip resistance increased when the modulus of compression increased. The radial stress increased nonlinearly when the critical stress ratio increased. However, the relationship between circumferential stress, tip resistance and critical stress ratio showed linear growth properties. When the penetration probe diameters are in the range of 1.75 to 2.95 mm, theoretical values are smaller than test data, and all the deviations between theoretical and test values are within 5%. Therefore, results indicate the elastoplastic solution can be used to predict the tip resistance and penetration stress.

Keywords: Elastoplastic solution · Spherical cavity expansion
Penetration resistance · Miniature penetrometer test

Notation:

M is the stress ratio of critical state line
λ is the hardening index
κ is the swelling index
p_0 is the present overburden stress or initial stress
a is the radius of cavity after expansion
p is the mean stress
u_r is the displacement in radius direction
r_0 is the initial radius position
r is the radius position

A. Zhou et al. (Eds.): GSIC 2018, *Proceedings of GeoShanghai 2018 International Conference: Fundamentals of Soil Behaviours*, pp. 919–928, 2018.
https://doi.org/10.1007/978-981-13-0125-4_102

σ_0 is the initial radial stress
σ_r is the radial stress
σ_θ is the circumferential stress
p_0 is the present overburden stress or initial stress
σ_p is the mean stress increment at the elastoplastic boundary
σ_r^a is the radial stress at radius of cavity after expansion
σ_θ^a is the circumferential stress at radius of cavity after expansion
ε_r is the radial strain
ε_θ is the circumferential strain
ε_r^p is the radial strain at the elastoplastic boundary
ε_θ^p is the circumferential strain at the elastoplastic boundary
μ is the Poisson's ratio
u_r is the displacement in radius direction
u_p is the displacement increment at the elastoplastic boundary
p is the mean stress
q is the difference between radial stress and circumferential stress
p_c is the preconsolidation pressure
p_0 is the present overburden stress or initial stress
β is the over consolidation ratio
e is the void ratio
e_0 is the initial void ratio
Q_p^r is the partial tip resistance at radial direction
Q_p^θ is the partial tip resistance at circumferential direction
Q_p is the tip resistance

1 Introduction

The miniature penetrometer tests are often used to investigate the distribution and strength of aggregates in soils. In this work, we are trying to use the cavity expansion method to describe the miniature penetration problems, since the process of probe penetration is similar to that of pile penetration. The cavity expansion method has been widely used in geotechnical engineering, particularly for pile driving and bearing capacity [1, 2], in laboratory or in-situ testing and numerical simulations [3–8]. However, the cavity expansion method is generally used based on the Mohr–Coulomb criterion [9], that is, soil is considered to be an ideal elastoplastic material. In this circumstance, soil failure is completely caused by shearing force, and the yield criterion will be used equal to the failure criterion, but practically, the yield in soil bodies is different from failure. Compared with the Mohr–Coulomb criterion, the modified Cambridge clay (MCC) model is preferred as the latter can take into account the plastic yield of soil in spherical stress [10, 11]. Schofield [12] and Roscoe [13] established a basic frame for the MCC model on the basis of critical state soil mechanics. And the MCC model can effectively represent the basic features of consolidated soil, such as strain-hardening and shear-contraction behaviors. The parameters λ, κ, and M, in the

MCC model are the commonly used geotechnical parameters that are applied to most leading soil elastoplastic constitutive models, including overconsolidated and structural constitutive models [14, 15]. In this work, the elastoplastic analysis of spherical cavity expansion was conducted using the MCC model.

2 Mathematical Model Building and Assumptions

The probe penetration by using the miniature penetrometer resulted in soil-squeezing, in which the pore forming process can be considered as a spherical cavity expansion process with downward movement. In the spherical expansion process, the soil in the spherical region around the spherical pore is transferring from an elastic state into a plastic state with increasing internal pressure. Different from the evident flow cracked zones caused by large diameter pile penetration into soil in engineering, the probe holes in the miniature penetrometer tests are smaller than the real pile diameters. Therefore, the flow cracked zones in the soil around probes was not taken into account, only plastic and elastic zones exist. The semispherical cavity expansion model of the plastic and elastic zones is shown in Fig. 1.

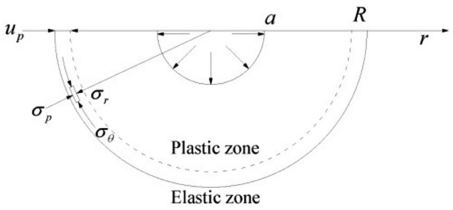

Fig. 1. Expansion of spherical cavity

The soil unit's initial aperture is zero, and p_0 is the initial average stress. After expansion, the end aperture is a (Fig. 1) and the average stress on any point is p. The soil unit radial displacement can be written as $u_r = r - r_0$. After expansion, the regions $(r > R)$ are elastic regions and its strain–stress relationship fulfills the generalized Hooke's law. The regions $(r \leq R)$ are plastic regions and volumetric changes of soil can be induced. The strain–stress relationship agrees with the MCC yielding model. Due to the fact that the diameters of miniature penetrometer probe are much smaller than the sample diameter, it can be assumed that the excess pore water pressure can be ignored during the whole pore expansion process of probe penetration.

3 Theoretical Derivation

Before soil expansion, we assume $\sigma_r = \sigma_\theta = \sigma_0$ and $p_0 = \sigma_0$. The strain at any point will change at any time and the soil elements still meet the equilibrium conditions during soil expansion:

$$\partial\sigma_r/\partial r + 2(\sigma_r - \sigma_\theta)/r = 0. \tag{1}$$

When the radial initial stress of one point is σ_0, according to the elastic theory and the initial stress in elastic zones, the solutions to its displacement yield:

$$\sigma_r = \sigma_0 + \left(\sigma_p - \sigma_0\right)(R/r)^3, \tag{2}$$

$$\sigma_\theta = \sigma_0 - \left(\sigma_p - \sigma_0\right)(R/r)^3/2, \tag{3}$$

$$u_r = \left(\sigma_p - \sigma_0\right)(R/r)^3 r/4G, \tag{4}$$

At the boundary of elasticity and plasticity $(r = R)$, both σ_r and σ_θ meet the yield conditions of the MCC model:

$$p^2 - pp_c + q^2/M^2 = 0. \tag{5}$$

At the point $r = R$, according to Eqs. (2), (3), and (5), the radial stress and displacement on the elastoplastic boundary are expressed as follows:

$$\sigma_p = \sigma_0 + 2Mp_0\sqrt{\beta - 1}/3, \tag{6}$$

$$u_p = Mp_0\sqrt{\beta - 1}R/6G. \tag{7}$$

During the soil expansion process, the plastic yield stress should meet:

$$q_y = Mp_0\sqrt{\beta - 1}. \tag{8}$$

According to the MCC model, we have

$$dq/dp = 2G\eta/E\left(M^2 - \eta^2\right). \tag{9}$$

When soil is in the yield condition, the stress at any point on the yield surface $\left(p_0, Mp_0\sqrt{\beta - 1}\right)$ meets Eq. (9), thus, Eq. (10) is obtained:

$$dq/dp = 2G\sqrt{\beta - 1}/EM(2 - \beta) \tag{10}$$

By integrating Eq. (10), the following equation is obtained:

$$q = Ap + B, \tag{11}$$

where

$$A = 2G\sqrt{\beta - 1}/EM(2 - \beta), \tag{12}$$

$$B = Mp_0\sqrt{\beta - 1} - 2Gp_0\sqrt{\beta - 1}/EM(2 - \beta) \tag{13}$$

Substituting $p = (\sigma_r + 2\sigma_\theta)/3$ and $q = \sigma_r - \sigma_\theta$ into Eq. (11), one can obtain:

$$f = \sigma_r + \gamma\sigma_\theta + \alpha = 0, \tag{14}$$

Where

$$\gamma = (2A + 3)/(A - 3), \alpha = 3B/(A - 3). \tag{15}$$

With the associated flow rule, we have

$$d\varepsilon_r^p = d\lambda \frac{\partial f}{\partial \sigma_r}, \tag{16}$$

$$2d\varepsilon_\theta^p = d\lambda \frac{\partial f}{\partial \sigma_\theta}. \tag{17}$$

From Eqs. (14), (16), and (17), the following equations can be obtained:

$$d\varepsilon_r^p / d\varepsilon_\theta^p = -2/\gamma, \tag{18}$$

$$d\sigma_\theta = -d\sigma_r/\gamma. \tag{19}$$

When $d\varepsilon_r^p = d\varepsilon_r - d\varepsilon_{re}$ and $d\varepsilon_\theta^p = d\varepsilon_\theta - d\varepsilon_{\theta e}$, the following equation is obtained combining with Eq. (18):

$$\gamma d\varepsilon_r + 2d\varepsilon_\theta = \gamma d\varepsilon_{re} + 2d\varepsilon_{\theta e}. \tag{20}$$

According to Hooke's law, we have

$$d\varepsilon_{re} = \frac{1}{E}\left(d\sigma_r - 2\mu d\sigma_\theta\right), \tag{21}$$

$$d\varepsilon_{\theta e} = \frac{1}{E}[(1 - \mu)d\sigma_\theta - \mu d\sigma_r]. \tag{22}$$

Substituting Eqs. (21), (22), and (19) into Eq. (20) yields:

$$d\varepsilon_r + \frac{2}{\gamma} d\varepsilon_\theta = \frac{\chi}{\gamma} d\sigma_r, \tag{23}$$

Where

$$\chi = \frac{1}{E}[\gamma - 2(1 - \mu)/\gamma]. \tag{24}$$

Integrating Eq. (23):

$$\varepsilon_r + 2\varepsilon_\theta/\gamma = \chi(\sigma_r - p_0)/\gamma. \tag{25}$$

The strain of soil in the plastic region agrees with large-deformation theory. According to the theory of plasticity, we have

$$\varepsilon_r = \ln\left(\frac{dr}{dr_0}\right), \varepsilon_\theta = \ln\left(\frac{r}{r_0}\right). \tag{26}$$

Deforming at $r_0 = r - u_r$ and combining with Eq. (26) yields:

$$\varepsilon_r = -\ln\left(1 - \frac{du_r}{dr}\right), \varepsilon_\theta = -\ln\left(1 - \frac{u_r}{r}\right). \tag{27}$$

Systemizing after substituting Eq. (27) into Eq. (25) produces:

$$1 - \frac{du_r}{dr} = e^{-\frac{\chi}{\gamma}(\sigma_r - p_0)}\left(1 - \frac{u_r}{r}\right)^{-\frac{2}{\gamma}}. \tag{28}$$

Given that the stress state of any point in the soil meets the equilibrium conditions, substituting Eq. (14) into Eq. (1) yields:

$$\frac{\partial \sigma_r}{\partial r} + 2\frac{(1 + 1/\gamma)\sigma_r + \alpha/\gamma}{r} = 0 \tag{29}$$

The solution to Eq. (29) is expressed as:

$$\sigma_r = A_1 + B_1\left(\frac{r}{R}\right)^C, \tag{30}$$

$$A_1 = -B/A, C = -2(1 + 1/\gamma) = \frac{-6A}{2A + 3}. \tag{31}$$

In Eq. (30), $r = R$. By combining Eq. (30) with Eq. (6), the following solution can be obtained:

$$B_1 = \sigma_0 + \frac{2Mp_0\sqrt{\beta - 1}}{3} - A_1. \tag{32}$$

Thus, by substituting Eq. (30) into the exponent part $e^{-\frac{\chi}{\gamma}(\sigma_r - p_0)}$ of Eq. (28), the deformation is expressed as:

$$e^{-\frac{\chi}{\gamma}(\sigma_r - p_0)} = e^{-\frac{\chi}{\gamma}\left(-\frac{B}{A} - p_0\right)}e^{-\frac{\chi}{\gamma}\left(\frac{B_1}{R^C}\right)r^C} = Ne^{Tr^C}. \tag{33}$$

Where

$$N = e^{-\frac{\chi}{\gamma}(A_1 - p_0)}, \tag{34}$$

$$T = -\frac{\chi}{\gamma R^C} B_1. \tag{35}$$

Thus, Eq. (28) can be read:

$$1 - \frac{du_r}{dr} = N e^{Tr^C} \left(1 - \frac{u_r}{r}\right)^{-\frac{2}{\gamma}}. \tag{36}$$

Combining Eqs. (7) and (36) yields:

$$u_r = r\left\{1 - \left\{\frac{1}{r}\left[R\left(1 - \frac{Mp_0\sqrt{\beta - 1}}{6G}\right)^{\frac{\gamma+2}{\gamma}} + \sum_{n=0}^{\infty} \frac{(\gamma+2)NT^n}{\gamma n!}\left(r^{nc} - R^{nc}\right)\right]\right\}^{\frac{\gamma}{\gamma+2}}\right\}. \tag{37}$$

When $r = a$, $u_r = a$, the solution to Eq. (37) is modified as:

$$\left[R\left(1 - \frac{Mp_0\sqrt{\beta - 1}}{6G}\right)^{\frac{\gamma+2}{\gamma}} + \sum_{n=0}^{\infty} \frac{(\gamma+2)NT^n}{\gamma n!}\left(a^{nC} - R^{nC}\right)\right] = 0. \tag{38}$$

Solution R can be obtained from Eq. (38). Generally, $n = 2$ can meet engineering demands, which is the radius of the plastic zone. Substituting Eq. (30) into Eq. (14) yields:

$$\sigma_\theta = A_1 - \frac{B_1}{\gamma}\left(\frac{r}{R}\right)^C. \tag{39}$$

With $r = a$ and considering Eqs. (30) and (39), the corresponding resistances are radical stress σ_r^a and tangential stress σ_θ^a as follows:

$$Q_p^r = \int_0^{2\pi}\int_0^{\pi/2} \sigma_r^a \cos(\phi) r^2 \sin(\phi) d\phi d\theta = \sigma_r^a \pi a^2, \tag{40}$$

$$Q_p^\theta = \int_0^{2\pi}\int_0^{\pi/2} \sigma_\theta^a \sin(\phi) r^2 \sin(\phi) d\phi d\theta = \sigma_\theta^a \pi^2 a^2/2. \tag{41}$$

Thus, the tip resistance effect caused by the combination of σ_r^a and σ_θ^a is expressed as follows:

$$Q_p = Q_p^r + Q_p^\theta = \pi a^2\left(\sigma_r^a + \sigma_\theta^a \pi/2\right). \tag{42}$$

Where Q_p is the theoretical value of tip resistance.

4 Verification

As previously mentioned, the elastoplastic solution to spherical cavity expansion for stress distribution in saturated clay is studied using cavity expansion theory in combination with the modified Cambridge clay model (MCC). In order to verify the accuracy of the solution, miniature penetrometer tests had been carried out.

A series of mechanical property tests under consolidation and triaxial compression conditions was conducted by the authors in [16]. Then the associated geotechnical parameters required in the model were obtained: hardening index $\lambda = 0.0577$, swelling index $\kappa = 0.0108$, modulus of compression $E_s = 4.5$ MPa preconsolidation pressure $p_c = 110.0$ kPa, initial stress $p_0 = 61.62$ kPa, over-consolidation ratio $\beta = 1.785$, effective cohesion $c' = 16.1$ kPa, effective friction angle $\varphi' = 25.5°$, critical stress ratio $M = 1.08$, initial void ratio $e_0 = 0.62$, specific volume $\Gamma = 1.62$.

The miniature penetrometer test device is shown in Fig. 2(a). Cylinder probes with the length of 60 mm were used in the test, and the diameters of the probes are 2.9, 2.65, 2.35, 2.05, and 1.75 mm, as shown in Fig. 2(b). The measured speed is 50.5 mm/min and the penetration depth is 8.0 mm.

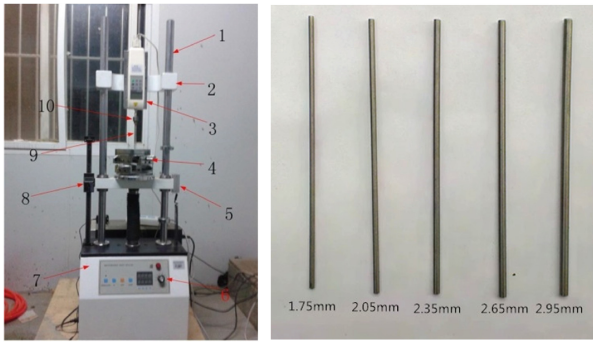

(a) (b)

Fig. 2. Miniature penetrometer and probes

According to Eq. (42), the values of different diametric probe penetration resistances and penetration stresses can be obtained (Table 1).

Table 1. Comparison between calculated and test data

Probe diameter (mm)	Calculated tip resistance (N)	Calculated penetration stress (MPa)	Measured penetration stress (MPa)	Deviation (%)
2.95	46.17	6.759	7.10	−4.78
2.65	37.29	6.765	7.09	−4.63
2.35	29.34	6.768	6.84	−1.06
2.05	22.35	6.774	6.88	−1.53
1.75	16.30	6.780	6.91	−1.95

Table 1 shows that the changes in penetration stress calculated for different diametric probes are small. Thus, the change of probe diameter has less influence on the penetration stress. This finding agrees with the test results. Make a comparison between the calculated and measured values of the penetration stress: when the penetration probe diameters are in the range of 1.75 to 2.95 mm, the calculated values are smaller than the measured values, and all the deviations between calculated and measured values are within 5%.

5 Conclusions

The elastoplastic solution of spherical cavity expansion for stress distribution in saturated clay is deduced using cavity expansion theory in combination with the MCC model. The results indicate that the elastoplastic solution can be used to predict the tip resistance. The solution can offer a theoretical basis for the subsequent study on the aggregate distribution of mechanical properties in clay.

The problem is that the modulus and Poisson's ratio keep unchanged in the calculation, which cause larger stress and deformation values compared with the test data. In addition, the MCC model is merely suitable for normally consolidated and light overconsolidated soil. Although the penetration stress calculated by the MCC model match well with the test value when the penetration speed is 50.5 mm/min, the penetration speeds are not considered in the MCC model. Therefore, further improvements on the MCC model are needed.

Acknowledgments. The financial supports from GuangXi Key Laboratory of Geomechanics and Geotechnical Engineering (14-KF-04) and Key Laboratory of Tianjin Soft Soil Character and Engineering Environment (Grant No. 2014SCEEKL01) are gratefully acknowledged.

References

1. Gibson, R.: Correspondence. Géotechnique **18**(2), 275–276 (1968)
2. Randolph, M.F., Carter, J., Wroth, C.: Driven piles in clay—the effects of installation and subsequent consolidation. Géotechnique **29**(4), 361–393 (1979)

3. Suzuki, Y., Lehane, B.M.: Analysis of CPT end resistance at variable penetration rates using the spherical cavity expansion method in normally consolidated soils. Comput. Geotech. **69**, 141–152 (2015)
4. Vesic, A.S.: Expansion of cavities in infinite soil mass. J. Soil Mech. Found. Div. **98**(3), 265–290 (1972)
5. Chai, J., Hossain, M.J., Carter, J., Shen, S.L.: Cone penetration-induced pore pressure distribution and dissipation. Comput. Geotech. **57**, 105–113 (2014)
6. Wang, S.Y., Chan, D.H., Lam, K.C., Au, S.K.A.: Numerical and experimental studies of pressure-controlled cavity expansion in completely decomposed granite soils of Hong Kong. Comput. Geotech. **37**(7), 977–990 (2010)
7. Tolooiyan, A., Gavin, K.: Modelling the cone penetration test in sand using cavity expansion and arbitrary lagrangian eulerian finite element methods. Comput. Geotech. **38**(4), 482–490 (2011)
8. Yu, H., Mitchell, J.: Analysis of cone resistance: review of methods. J. Geo. Geoenviron. Eng. **124**(2), 140–149 (1998)
9. Carter, J., Booker, J., Yeung, S.: Cavity expansion in cohesive frictional soils. Géotechnique **36**(3), 349–358 (1986)
10. Cao, L.F., Teh, C.I., Chang, M.F.: Undrained cavity expansion in modified cam clay I: theoretical analysis. Géotechnique **51**(4), 323–334 (2001)
11. Chang, M.F., Teh, C.I., Cao, L.F.: Undrained cavity expansion in modified cam clay II: application to the interpretation of the piezocone test. Géotechnique **51**(4), 335–350 (2001)
12. Schofield, A., Wroth, P.: Critical State Soil Mechanics, pp. 93–114. Mcgraw-Hill, London (1968)
13. Roscoe, K., Schofield, A., Thurairajah, A.: Yield of clays in states wetter than critical. Géotechnique **13**(3), 211–240 (1963)
14. Yao, Y., Hou, W., Zhou, A.: UH model: three-dimensional unified hardening model for overconsolidated clays. Géotechnique **59**(5), 451–469 (2009)
15. Pender, M.: A model for the behaviour of over consolidated soil. Géotechnique **28**(1), 1–25 (1978)
16. Kong, L.W., Zhou, B.C., Bai, H., Chen, W.: Experimental study of deformation and strength characteristics of Jingmen unsaturated expansive soil. Rock Soil Mech. **31**(10), 3036–3042 (2010)